International Journal of Pharmaceutics 360 (2008) 177–183

Contents lists available at ScienceDirect

International Journal of Pharmaceutics

journal homepage: www.elsevier.com/locate/ijpharm

Pharmaceutical Nanotechnology

Solid lipid nanoparticles for retinal gene therapy: Transfection and intracellular trafficking in RPE cells

A. del Pozo-Rodríguez, D. Delgado, M.A. Solinís, A.R. Gascón, J.L. Pedraz*

Pharmacy and Pharmaceutical Technology Laboratory, Faculty of Pharmacy, University of the Basque Country (UPV-EHU), Paseo de la Universidad 7, 01006 Vitoria-Gasteiz, Spain

ARTICLE INFO

Article history:
Received 13 February 2008
Received in revised form 3 April 2008
Accepted 5 April 2008
Available online 22 April 2008

Keywords:
Solid lipid nanoparticles
Transfection
Intracellular trafficking
ARPE-19 cells
Caveolae
Clathrin

ABSTRACT

Retinal pigment epithelial (RPE) cells are usually employed to study DNA systems for diseases related to problems in the retina. Solid lipid nanoparticles (SLNs) have been shown to be useful non-viral vectors for gene therapy. The objective of this work was to evaluate the transfection capacity of SLNs in the human retinal pigment epithelial established cell line (ARPE-19) in order to elucidate the potential application of this vector in the treatment of retinal diseases. Results showed a lower transfection level of SLNs in ARPE-19 cells than in HEK293 (2.5% vs. 14.9% EGFP positive cells at 72 h post-transfection). Trafficking studies revealed a delay in cell uptake of the vectors in ARPE-19 cells. Differences in internalization process into the two cell lines studied explain, in part, the difference in the gene expression. The clathrin-mediated endocytosis in ARPE-19 cells directs the solid lipid nanoparticles to lysosomes; moreover, the low division rate of this cell line hampers the entrance of DNA into the nucleus. The knowledge of intracellular trafficking is very useful in order to design more efficient vectors taking into account the characteristics of the specific cell line to be transfected.

1. Introduction

Nowadays multiple diseases may be the object of gene therapy, from monogenic diseases such as cystic fibrosis (Davies, 2006) to more complex diseases such as cancer (Brandwijk et al., 2007), and specifically those related to ocular disorders are attracting increasing interest. The eye is a promising organ for gene therapy because of its well-defined anatomy, immunoprivilege and accessibility. Furthermore, as the media is transparent, the gene transfer process can be easily seen (Liu et al., 2007). Gene therapy with viral vectors has been proved to be an efficient treatment for some retina related diseases, such as Leber congenital amaurosis (Bemelmans et al., 2006; Bennicelli et al., 2008) or X-linked juvenile retinoschisis (Min et al., 2005). Retinal pigment epithelial (RPE) cells are usually employed "in vitro" (Chaum et al., 2000; Doi et al., 2002; Pitkanen et al., 2004; Mannisto et al., 2005; Bejjani et al., 2005) as a tool to evaluate new therapeutic strategies in gene therapy for retinal diseases.

Non-viral vectors are being extensively studied in gene therapy as an attractive alternative to viral-based systems due to the reduction of risks such as oncogenicity or immunogenicity, their easier manufacture and the absence of DNA size limit. However, their clinical use requires improvement in terms of effectiveness, which depends not only on the administration system but also on the targeted cells.

It is known that transfection is conditioned by the entry and posterior intracellular trafficking of the vectors and these processes are cell line dependent (Li et al., 2004; von Gersdorff et al., 2006). Fig. 1 illustrates the barriers that DNA delivery systems have to overcome during the trafficking to the nucleus before the synthesis of the encoded protein. First, vectors have to bind to cell surface, which occurs by electrostatic interactions between the positively charged systems and the negative charges of the cell membrane. The next step consists in the entry into the cell, with endocytosis as the main process postulated (Zabner et al., 1995; Zuhorn et al., 2002; Rejman et al., 2005). Once inside the cell, the DNA has to cross the nuclear envelope to reach the cellular machinery for protein synthesis.

Cationic lipid-based systems formulated as liposomes, solid lipid nanoparticles (SLNs) or emulsions (Liu et al., 1996; Olbrich et al., 2001; Kim et al., 2002; Tabatt et al., 2004; Salvati et al., 2006), are included in the group of non-viral systems for DNA delivery. In the last years SLNs have attempted a big development as drug delivery systems, but there are still few papers about their use in gene therapy. However, the publications about the use of cationic liposomes in this field are numerous, although by now no formulation has been marketed for nucleic acid delivery. From the point of view of application, SLNs have good stability (Freitas and Müller, 1999),

* Corresponding author. Tel.: +34 945013091; fax: +34 945013040.
E-mail address: joseluis.pedraz@ehu.es (J.L. Pedraz).

0378-5173/$ – see front matter © 2008 Elsevier B.V. All rights reserved.
doi:10.1016/j.ijpharm.2008.04.023

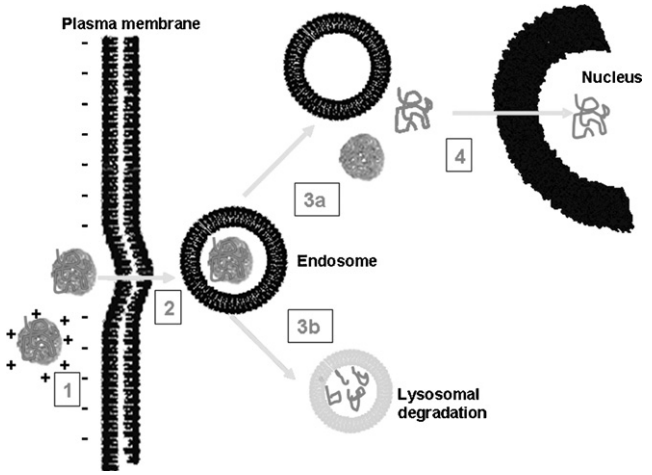

Fig. 1. Trafficking of non-viral vectors during the transfection process. (1) Binding to plasma membrane due to electrostatic interactions between the positive charged vectors and the negative charges of the plasma membrane. (2) Entry into the cell: endocytosis has been established as the main entry mechanism. (3a) Displacement of the endosomes to the proximity of the nucleus and release of the vectors to the cytoplasm. (3b) The exit of vectors from endosomes has to take place before the fusion with lysosomes, which possess enzymes with ability to digest DNA. (4) Entry of DNA into the nucleus. This step can occur through pores in nuclear envelope or during mitosis, when the nuclear membrane is disrupted.

which facilitates the industrial elaboration and the manipulation for different processes such as lyophilization and they can be a promising alternative to the liposomes. We have already shown that SLNs composed by Precirol® ATO 5 as core lipid, DOTAP as cationic lipid and Tween 80 as tensioactive transfect the plasmid encoding the enhanced green fluorescent protein (pCMS-EGFP) in Human Embrionic Kidney (HEK293) culture cells (del Pozo-Rodriguez et al., 2007). This cell line is usually employed in "in vitro" transfection studies because its culture conditions and manipulation are optimized, and it is one of the best transfected cell lines, which makes it a good model for "in vitro" transfection studies. The objective of this work was to evaluate the transfection capacity of SLNs in the human retinal pigment epithelial established cell line (ARPE-19) in order to elucidate the potential application of this vector in the treatment of retinal diseases. Due to the importance of the cell uptake and the intracellular behaviour of the vectors we have studied the intracellular trafficking of the SLNs in ARPE-19 and HEK293 cells.

2. Materials and methods

2.1. Materials

Precirol® ATO 5 was provided by Gattefossé (Madrid, Spain). *N*-[1-(2,3-Dioleoyloxy) propyl]-*N*,*N*,*N*-trimethylammonium chloride (DOTAP), antibiotic/antimycotic and Nile Red were purchased from Sigma–Aldrich (Madrid, Spain). Tween 80 was provided by Vencaser (Bilbao, Spain) and dichloromethane by Panreac (Barcelona, Spain).

Plasmid pCMS-EGFP encoding the enhanced green fluorescent protein (EGFP) was purchased from BD Biosciences Clontech (Palo Alto, USA) and amplified by Dro S.L. (San Sebastián, Spain). The labelling of the plasmid pCMS-EGFP with ethidium monoazide (EMA) was also carried out by Dro S.L. (San Sebastián, Spain).

Hoechst 33258, AlexaFluor488-Cholera toxin and AlexaFluor488 Transferrin were provided by Molecular Probes (Barcelona, Spain), and Fluoromount G from SouthernBiotech (Coultek, España).

Cell culture reagents were purchased from LGC Promochem (Barcelona, Spain). Antibiotic Normocin™ was acquired from InvivoGen (San Diego, CA).

2.2. Preparation of SLN-DNA vectors

The SLNs were produced by a solvent emulsification/evaporation technique (Mehnert and Mader, 2001). The lipid Precirol® ATO 5 was dissolved in the organic solvent dichloromethane (5%, w/v), and then emulsified in an aqueous phase containing the cationic lipid DOTAP (0.4%, w/v) and the surfactant Tween 80 (0.1%, w/v). The organic phase/aqueous phase ratio was 1/5. The emulsion was obtained by sonication (Branson Sonifier 250, Danbury) during 30 s at 50 W. The organic solvent then was removed from the emulsion by evaporation using a magnetic agitator for 45 min followed by vacuum conditions for 15 min. Upon dichloromethane evaporation SLNs suspension was formed by precipitation of the Precirol® ATO 5 in the aqueous medium. Finally, SLNs were washed by centrifugation (3000 rpm, 20 min, 3 times) using the Amicon® Ultra centrifugal filters (Millipore, Madrid, Spain).

To prepare SLN-DNA complexes, a solution of pCMS-EGFP plasmid was mixed with the SLNs suspension. The ratio SLN/DNA, expressed as DOTAP/DNA ratio (w/w), was 5/1.

In order to analyze the trafficking of the vectors, SLNs were labelled with Nile Red (λ = 590 nm), and the plasmid pCMS-EGFP with ethidium monoazide (EMA; λ = 625 nm). The label of the SLNs was based on a method reported by Lombardi Borgia et al. (2005) to prepare Nile Red loading nanoparticular systems. SLNs were prepared by the emulsification/evaporation technique described above, incorporating the Nile Red in the dichloromethane. The plasmid was labelled according to the procedure described by Ruponen et al. (2001). One volume of ethidium monoazide bromide (Sigma–Aldrich) at 10 μg/ml in water was added to one volume of pCMS-EGFP at 400 μg/ml in water and the mixture was incubated for 1 h at room temperature in darkness. After the incubation period, the solution was exposed to UV light for 5 min. Gel filtration on NAP-25 Column (GE Healthcare) was used to purify the labeled DNA from free EMA. To remove intercalated but not covalently bound EMA, CsCl was added to a concentration of 1.1 g/ml and was gently mixed until it dissolved. Plasmid was extracted with CsCl-saturated isopropanol. The isopropanol washing step was repeated until the upper phase appeared clear. CsCl was removed by dialysis against water, and the labeled EMA-pCMS-EGFP plasmid was recovered with isopropanol precipitation.

2.3. Size and zeta potential measurements

The sizes of SLNs and SLN-DNA complexes were determined by photon correlation spectroscopy (PCS). Zeta potential was measured by laser doppler velocimetry (LDV). Both measurements were performed on a Malvern Zetasizer 3000 (Malvern Instruments, Worcestershire, UK). All samples were diluted in NaCl 0.1 mM.

2.4. Cell culture and transfection protocol

In vitro assays were performed with two different cell lines: human embryonic kidney (HEK293) cell line and human retinal pigmented epithelial (ARPE-19) cell line, obtained from the American Type Culture Collection (ATCC).

HEK293 cells were maintained in Eagle's Minimal Essential medium with Earle's BSS and 2 mM L-glutamine (EMEM) supplemented with 10% heat-inactivated horse serum and 1% antibiotic/antimycotic. Cells were incubated at 37 °C with 5% CO_2 in air and subcultured every 2–3 days using trypsin/EDTA. For trans-

fection HEK293 cells were seeded on 24 well plates at a density of 150,000 cells per well and allowed to adhere overnight.

ARPE-19 cells were maintained in Dulbecco's Modified Eagle's Medium/Han's Nutrient Mixture F-12 (1:1) medium (D-MEM/F-12) supplemented with 10% heat-inactivated fetal calf serum and 1% antibiotic solution Normocin™. Cells were incubated at 37 °C with 5% CO_2 in air and subcultured every 2–3 days using trypsin/EDTA. For transfection ARPE-19 cells were seeded on 12 well plates at a density of 30,000 cells per well and allowed to adhere overnight.

Seventy-five microliters of the vectors solution diluted in HBS (2.5 μg DNA) were added to each well, and cells were incubated with the vectors for 4 h at 37 °C. After that time the medium containing the complexes in the wells was diluted with 1 ml of complete medium and cells were allowed to grow for further 72 h.

2.5. Flow cytometry mediated analysis of transfection efficacy

At the end of the incubation period, the cells were washed once with 300 μl of PBS and were detached with 300 μl of 0.05% trypsin/EDTA. Then the cells were centrifuged at 1500 × *g* and the supernatant was discarded. Cells were resuspended with PBS and directly introduced to a FACSCalibur flow cytometer (Becton Dickinson Biosciences, San Jose, USA). Fluorescence of EGFP was collected at 525 nm (FL1). For each sample 10,000 events were collected.

2.6. Cellular uptake of non-viral vectors

Entry of vectors to the cells was studied quantitatively by flow cytometry and qualitatively by confocal laser scanning microscopy (CLSM). For this purpose SLNs were labelled with the fluorescent dye Nile Red (λ = 590 nm).

Cells incorporating vectors were quantified by flow cytometry at 650 nm (FL3) after detachment from plates at different time points. For each sample 10,000 events were collected.

For the CLSM study, cells were seeded in coverslips containing plates and treated with the vectors. At different incubation times, the medium was removed and cells were washed with PBS and fixed with paraformaldehyde 4%. We had previously checked that paraformaldehyde did not interact with the fluorescence of Nile Red or EGFP. Preparations were mounted on Fluoromount G and after air-drying images were obtained with an Olympus Fluoview FV500 confocal microscope using sequential acquisition to avoid overlapping of fluorescent emission spectra. CLSM images were captured in the General Service of Analytical Microscopy and High Resolution in Biomedicine of the University of the Basque Country (UPV-EHU).

2.7. Colocalisation assay

In order to identify the specific endocytic processes involved in the non-viral systems internalization cells were seeded in coverslips and co-incubated for 1 h with Nile Red labelled vectors and either AlexaFluor488-Cholera toxin (10 μg/ml) or AlexaFluor488-Transferrin (50 μg/ml), which are markers for caveolae-mediated endocytosis and clathrin-mediated endocytosis, respectively. Cell fixation and images acquisition were performed as described in Section 2.6.

2.8. Detection of intracellular EMA-labelled DNA by fluorescence microscopy

In order to evaluate the trafficking of DNA in the cytoplasm, cells were seeded in culture plates and treated with vectors containing pCMS-EGFP labelled with ethidium monoazide (EMA). Prior to the observation of the samples through the microscope, nucleuses were labelled with Hoechst 33258. Images were captured with an inverted microscopy equipped with an attachment for fluorescent observation (model EclipseTE2000-S, Nikon). Observations and image captures were performed using a 20× objective.

Table 1
Size and zeta potential of SLN-DNA vectors

	SLN-GFP	Nile-GFP	SLN-EMA
Size (nm)	281 (69)	269 (69)	222 (5)
Z potential (mV)	+30 (1)	+29 (1)	+30 (2)

SLN-GFP: vectors composed by non-labelled SLNs and non-labelled plasmid. Nile-GFP: vectors composed by Nile Red-labelled SLNs and non-labelled plasmid. SLN-EMA: vectors composed by non-labelled SLNs and EMA-labelled plasmid. SLN/DNA ratio 5/1 (w/w). Mean (SD: standard deviation) ($n = 3$).

2.9. Statistical analysis

Results are reported as means (SD = standard deviation). The statistical analysis was carried out with SPSS 14.0 for Windows® (SPSS®, Chicago, USA). Normal distribution of samples was assessed by the Shapiro–Wilk's test, and homogeneity of the variance by the Levene's test. The statistical analysis between HEK293 and ARPE-19 cells was determined with a Student's *t*-test. Differences were considered statistically significant if $p < 0.05$.

3. Results

3.1. Characterization of vectors: size and zeta potential

Table 1 summarizes the size and zeta potential of the vectors employed in this work. The positive charge allows vectors to bind to the negative charged cell surface and particle size influences the mechanism of cell internalization (Rejman et al., 2004). Results show that neither the Nile Red nor the ethidium monoazide (EMA) induced changes in particle size or zeta potential of SLN-DNA vectors ($p > 0.05$).

3.2. Transfection levels in culture cells

The transfection capacity of SLN-DNA vectors in HEK293 and ARPE-19 cells was evaluated. The percentages of cells expressing EGFP were measured at different times from 0.5 to 72 h after the addition of the vectors. Bars in Fig. 2 represent those levels. Results show that in HEK293 culture cells (white bars) green fluorescence was detected from 24 h, while in ARPE-19 cells (grey bars) green

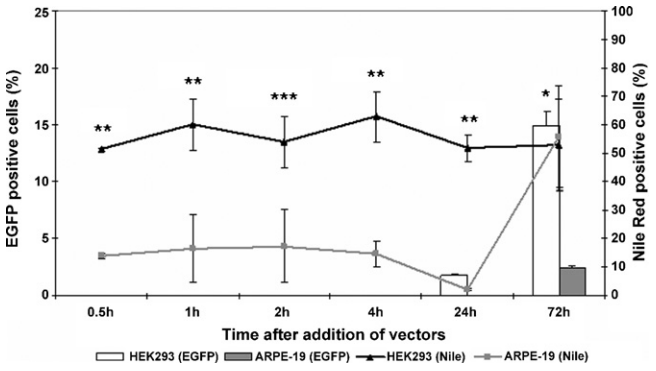

Fig. 2. Transfection and uptake of non-viral vectors by HEK293 and ARPE-19 cells. Bars represent the percentage of transfected cells in HEK293 (white bars) and in ARPE-19 cultures (grey bars). Lines represent the percentage of cells bearing vectors in HEK293 (black line) and ARPE-19 cultures (grey line). SLN/DNA ratio (w/w) was 5/1. Error bars represent SD ($n = 3$). *$p < 0.01$ in transfection against to ARPE-19 cells. **$p < 0.01$ in uptake against to ARPE-19 cells. ***$p < 0.05$ in uptake against to ARPE-19 cells.

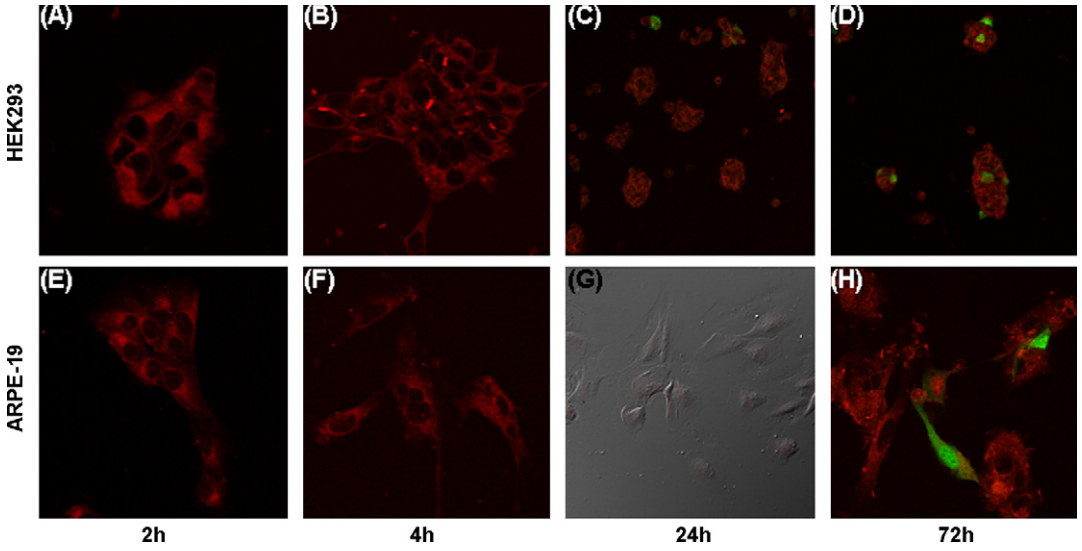

Fig. 3. Confocal images of HEK293 cells (A)–(D) and ARPE-19 cells (E)–(H) at different times after the addition of SLN-DNA vectors. (A) and (E) 2 h; (B) and (F) 4 h; (C) and (G) 24 h; (D) and (H): 72 h. Image in panel G was captured with transmitted light in order to evidence the lack of fluorescent cells. Cells were treated with Nile Red-labelled SLN-DNA vectors (red) carrying the plasmid pCMS-EGFP, which encodes EGFP (green). SLN/DNA ratio (w/w) 5/1.

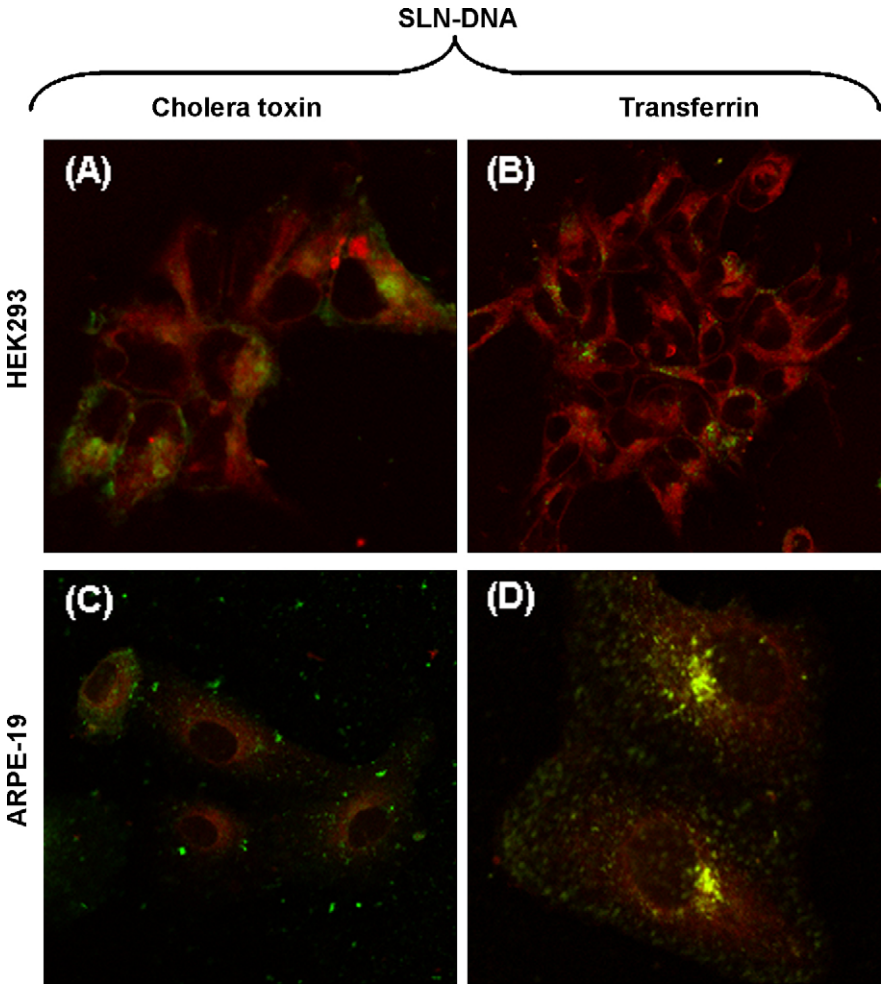

Fig. 4. CLSM images of HEK293 cells (A) and B) and ARPE-19 cells (C) and (D) coincubated for 1 h with Nile Red-labelled SLN-DNA vectors (red) and AlexaFluor 488-Cholera toxin (green) at 10 μg/ml (A) and (C) or AlexaFluor 488-Transferrin (green) at 50 μg/ml (B) and (D). SLN/DNA ratio (w/w) was 5/1.

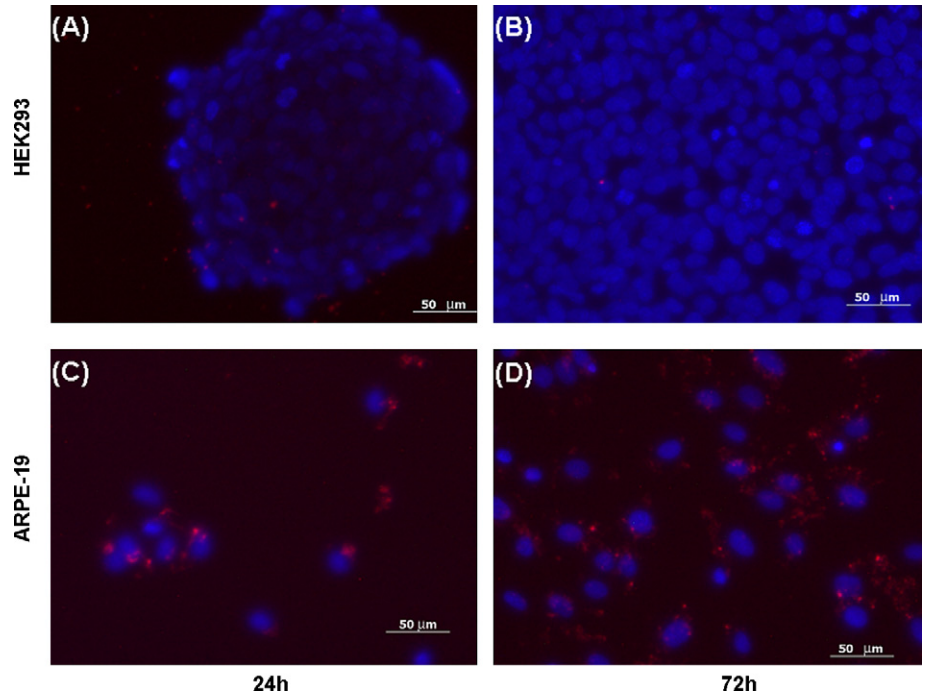

Fig. 5. Fluorescence microscopy images of HEK293 cells (A) and (B) and ARPE-19 cells (C) and (D) at different times after the addition of SLN-DNA vectors. (A) and (C) 24 h; (B) and (D) 72 h. Cells were treated with Hoechst 33258 in order to detect the nucleus (blue) and vectors containing EMA-labelled pCMS-EGFP plasmid (red). SLN/DNA ratio (w/w) 5/1.

fluorescence was only detected at 72 h. Moreover, transfection levels in HEK293 (14.9% EGFP positive cells) were higher ($p < 0.01$) than in ARPE-19 cells (2.5% EGFP positive cells).

3.3. Cell uptake and intracellular distribution of Nile Red-labelled vectors

In order to evaluate the entry of the vectors into the cells SLNs were labelled with Nile Red, and they were bound to non-labelled plasmid. We compared the percentage of Nile Red positive HEK293 and ARPE-19 cells by flow cytometry. The lines in Fig. 2 feature the results. In HEK293 cells levels were higher and did not vary along time; between 50% and 60% of the cells showed red fluorescence during the 72 h the experiment lasted. In ARPE-19 cells, during the first 4 h the percentage of Nile Red positive cells ranged from 10% to 20%, and at 72 h, cells containing nanoparticles increased to 55.8%, similar to the uptake level detected in HEK293 cells.

Fig. 3 summarizes CLSM images captured from 2 to 72 h after the addition of vectors to the cells. After 2 h HEK293 cells (Fig. 3A) showed vectors distributed homogenously in all the cytoplasm. However, in ARPE-19 cells (Fig. 3E) red fluorescence was mainly observed near the nucleus, in the region corresponding to the endoplasmic reticulum. At 4 h, in the two cell lines vectors were distributed around the nucleus. Twenty-four hours after the addition of the vectors EGFP (green fluorescence) was only detected in HEK293 cultures (Fig. 3C). Finally, at 72 h both cell lines showed EGFP and red fluorescence (Fig. 3D and H). In ARPE-19 cells fluorescence of the vectors was very intense and appeared homogeneously distributed in the cytoplasm.

3.4. Colocalisation assay

We also studied vectors entry mechanism in each cell line by CLSM. Colocalisation studies of vectors with Alexa Fluor 488-labelled Transferrin and Cholera Toxin (Fig. 4) indicated that SLN-DNA vectors showed colocalisation with Cholera Toxin in HEK293 cells and with Transferrin in ARPE-19 cells. These findings indicate that in retinal cells SLN-DNA vectors mainly entered by clathrin-mediated endocytosis and in HEK293 they entered via caveolae.

3.5. Intracellular distribution of EMA-labelled DNA in culture cells

In order to study the behaviour of DNA into the cells we employed the plasmid pCMS-EGFP labelled with ethidium monoazide (EMA) to elaborate SLN-DNA vectors. We also treated cells with Hoechst 33258 for the localization of the nucleus. Fig. 5 represents images captured by fluorescence microscopy at 24 h after the addition of the vectors. At 72 h HEK293 cells hardly showed any red fluorescence (Fig. 5B), while in ARPE-19 cells (Fig. 5D) the presence of labelled DNA increased with respect to observations at 24 h.

4. Discussion

The transfection capacity of solid lipid nanoparticles (SLNs), composed by Precirol® ATO 5, DOTAP and Tween 80 (del Pozo-Rodriguez et al., 2007) has been evaluated in the human retinal pigment epithelial established cell line (ARPE-19). The flow cytometry study (bars in Fig. 2) showed that SLNs are able to transfect ARPE-19 cells although transfection levels were lower than in HEK293 cells (2.5% vs. 14.9% EGFP positive cells at 72 h). In order to find the reason for the low transfection level in ARPE-19 cells, we performed a trafficking study of the SLNs in both cell lines.

Firstly, we studied the entry of Nile Red-labelled vectors by flow cytometry. In Fig. 2 (lines) we can observe that at 0.5 h after the addition of the vectors, 50% of the HEK293 cells contained vectors, and this level was maintained until 72 h. In ARPE-19 cells, during the first 4 h positive cells ranged from 10% to 20%, and at 72 h, cells containing nanoparticles increased to 55.8%, a level similar to the

uptake observed in HEK293 cells. Based on these results, a delay in transfection in ARPE-19 cells with respect to the HEK293 cells is expected. Transfection levels (Fig. 2, bars) confirmed this delay. Green fluorescence was detected at 24 h in HEK293 cells, but in ARPE-19 cells, green fluorescence was not observed until 72 h.

Once the vector is inside the cells, the transport of DNA through the cytoplasm to the nucleus also plays an important role on transfection. The mobility of DNA molecules is difficult due to their large size and they can be degraded by cytoplasmic components. SLNs condense the DNA and reduce its size to facilitate the mobility and protection of the plasmid from components such as DNases (del Pozo-Rodriguez et al., 2007).

The intracellular processing of the complex and its intracellular fate is affected by the pathway of entry into the cells. Endocytosis has been postulated as the main mechanism of entry for non-viral systems. Multiple mechanisms of endocytosis have been described, such as phagocytosis, pynocytosis, clathrin-mediated and caveolae-mediated. The relative contribution of each pathway in the lipoplex internalization has been poorly defined to date, although clathrin-mediated endocytosis has been described as the main pathway for cationic lipid-based systems, and specifically, for lipoplexes composed by the cationic lipid DOTAP and DNA. Rejman et al. (2005, 2006) concluded that the uptake occurs solely by the clathrin-mediated mechanism.

Clathrin-mediated endocytosis leads to an intracellular pathway in which endosomes fuse with lysosomes degrading their content, whereas caveolae-mediated endocytosis avoids the lysosomal pathway and vector degradation. Hence, a timely release of the DNA from the endosomal compartment is essential in the clathrin pathway. Hoekstra et al. (2007) have studied the endosomal escape of cationic lipid vectors and they describe that the non-lamellar phase changes of the lipoplexes, facilitated by intracellular lipids, allow DNA to dissociate from the vector and destabilize endosomal membranes.

Confocal images in Fig. 3 feature the intracellular disposition of the SLN-DNA vectors in HEK293 (A)–(D) and ARPE-19 cells (E)–(H). In HEK293 cells (Fig. 3A) red fluorescence was homogenously dispersed, indicating that vectors were taking up almost all the cytoplasm. However, in retinal cells (Fig. 3E) vectors were mainly located in the same region that the rough endoplasmic reticulum and the Golgi apparatus, where lysosomes are produced. Thus, in ARPE-19 cells, the exposure of vectors to lysosomal digestive enzymes seems to be higher than in HEK293. Although SLNs are expected to entry by clathrin-mediated endocytosis as described for other lipid systems, differences observed in the intracellular localization between the two cell lines may be due to differences in the uptake mechanism: clathrin-mediated endocytosis in ARPE-19 cells vs. caveolae-mediated in HEK293 cells.

In order to confirm the previous hypothesis, colocalization studies were carried out with Alexa Fluor 488-Cholera toxin and Alexa Fluor 488-Transferrin, which are markers for caveolae-mediated endocytosis and clathrin mediated endocytosis, respectively (Pelkmans and Helenius, 2002; Pujals et al., 2008). Results presented in Fig. 4 revealed that SLN-DNA vectors colocalize with Cholera Toxin in HEK293 cells and mainly with Transferrin in ARPE-19 cells. These findings confirmed that SLN-DNA vectors mainly entered retinal cells by clathrin-mediated endocytosis and only via caveolae in HEK293. A higher clathrin-dependent entry and later internalization process in the ARPE-19 cell line compared to HEK293 cells may justify, in part, the lower transfection of the vectors in retinal cells.

Douglas et al. (2008) studied the transfection of alginate-quitosan nanoparticles in different cell lines and concluded that clathrin-mediated internalization is required for efficient transfection: complexes that entered cells through caveolae-mediated processes were not trafficked to the endolysosomal pathway and, thus, were unable to escape from the vesicles and remained trapped and ineffective for transfection. However, our lipidic nanoparticles were able to transfect HEK293 cells in spite of their internalization into cells via caveolae. This indicates a successful escape from the caveosomes. It is known that the internalization process depends on the cell line but the composition of the formulation also conditions the endocytosis mechanism. Rejman et al. (2004) and Kanatani et al. (2006) also showed transfection via caveolea with polyplexes and lipofectamine, respectively. The knowledge of the endocytosis mechanisms should help us to design more efficient formulations. On the one hand, the entrance mechanism could be targeted to caveolae to prevent lysosomal degradation; on the other hand, the endosome escape can be favoured in the case of clathrin-mediated endocytosis. The use of additives as peptides (Foerg et al., 2005; Pujals et al., 2008) favours the cell uptake via caveolae and the incorporation of co-lipids as DOPE or cholesterol (Karmali and Chaudhuri, 2007) helps endosome escape. Further similar research studies using other cell lines would ensure and reinforce the findings reported here.

Before entering into the nucleus, the DNA must be released from the complexes and this may be one of the most crucial steps for transfection. The capacity of the vector to condensate the DNA conditions its release profile. In a previous study (del Pozo-Rodriguez et al., 2007) we showed that the DNA was able to be released from the SLN. The entry into the nucleus is in general quite difficult, as the nuclear membrane is a selective barrier to molecules bigger than 40 kDa, and plasmids surpass that size. There are two mechanisms those molecules can use to overcome that barrier: the disruption of the nuclear membrane during mitosis or the import through nuclear pore complex (NPC). This latter mechanism requires nuclear localization signals (NLS), which can be used to improve transfection by non-viral vectors (Boulanger et al., 2005). Since our vectors do not have any NLS, plasmid DNA will enter the nucleus only during mitosis when the nuclear membrane transiently disappears. The division of HEK293 cells is faster than in ARPE-19 cells (Thomas and Smart, 2005); therefore, the entry of plasmid into the nucleus will be more difficult in ARPE-19 cells. The importance of division rate on the transfection process for cationic lipid-based systems has been already demonstrated (Mortimer et al., 1999; Tseng et al., 1999). The slower division rate of ARPE-19 cells induces a delay in the entry of the DNA into their nucleus and the transduction will occur later. Therefore, the delay observed in the protein expression in ARPE-19 cells with respect to HEK293 cells (Fig. 2) will be due not only to a delay in the entrance of the vector into the cell but also to a slower division rate.

In Fig. 5 we can see the distribution of the DNA inside the cell by using vectors containing DNA labelled with ethidium monoazide (EMA), a red fluorescent DNA intercalating agent. In ARPE-19 cells, unlike in HEK293 cells, red fluorescence was higher at 72 h than at 24 h, and the DNA was close to the nucleus. As mentioned above, this is explained by a delay in the internalization uptake and also due to a slower cell division. These results made us think that in this cell line transfection will take a longer time than in HEK293. However, we tested transfection at day 7 (data not shown) and transfection decreased. This could be explained because the DNA stayed longer in the cytoplasm and was more exposed to degradation by different cytoplasmic agents such as DNAses. NLS can be incorporated into the DNA complexes in order to direct the plasmid into the nucleus, shortening the stay of the plasmid in the cytoplasm and hence, decreasing DNA degradation. Subramanian et al. (1999) reported an increase from 5% to 80% in transfection of non-dividing cells by the incorporation of NLS in their lipoplexes.

In conclusion, differences in internalization of the vectors into the two cell lines explain, in part, the difference in the gene

expression. The lower transfection level obtained with the SLNs in ARPE-19 cells is due mainly to the cell uptake by a clathrin mediated endocytosis that directs the solid lipid nanoparticles to lysosomes; moreover, the low division rate hampers the entrance of DNA into the nucleus. The study of the intracellular trafficking is a very useful tool for the designing of more efficient vectors taking into account the characteristics of the specific cell line to be transfected.

Acknowledgements

We would like to thank the Spanish Ministry of Education and Science for research grant (AP2003-4780) awarded to Ana del Pozo. Authors also acknowledge the General Service of Analytical Microscopy and High Resolution in Biomedicine of the University of the Basque Country (UPV-EHU) for technical advice on confocal microscopy.

References

Bejjani, R., Benezra, D., Cohen, H., Rieger, J., Andrieu, C., Jeanny, J.C., Gollomb, G., Behar-Cohen, F., 2005. Nanoparticles for gene delivery to retinal pigment epithelial cells. Mol. Vis. 11, 124–132.

Bemelmans, A.P., Kostic, C., Crippa, S.V., Hauswirth, W.W., Lem, J., Munier, F.L., Seeliger, M.W., Wenzel, A., Arsenijevic, Y., 2006. Lentiviral gene transfer of Rpe65 rescues survival and function of cones in a mouse model of Leber congenital amaurosis. PLoS Med. 3, 1892–1903.

Bennicelli, J., Wright, J.F., Komaromy, A., Jacobs, J.B., Hauck, B., Zelenaia, O., Mingozzi, F., Hui, D., Chung, D., Rex, T.S., Wei, Z., Qu, G., Zhou, S., Zeiss, C., Arruda, V.R., Acland, G.M., Dell'Osso, L.F., High, K.A., Maguire, A.M., Bennett, J., 2008. Reversal of blindness in animal models of leber congenital amaurosis using optimized AAV2-mediated gene transfer. Mol. Ther. 16, 458–465.

Boulanger, C., Di Giorgio, C., Vierling, P., 2005. Synthesis of acridine-nuclear localization signal (NLS) conjugates and evaluation of their impact on lipoplex and polyplex-based transfection. Eur. J. Med. Chem. 40, 1295–1306.

Brandwijk, R.J.M.G., Griffioen, A.W., Thijssen, V.L.J.L., 2007. Targeted gene-delivery strategies for angiostatic cancer treatment. Trends Mol. Med. 13, 200–209.

Chaum, E., Hatton, M.P., Stein, G., 2000. Polyplex-mediated gene transfer into human retinal pigment epithelial cells in vitro. J. Cell. Biochem. 76, 153–160.

Davies, J.C., 2006. Gene and cell therapy for cystic fibrosis. Paediatr. Respir. Rev. 7, S163–S165.

del Pozo-Rodriguez, A., Delgado, D., Solinis, M.A., Gascon, A.R., Pedraz, J.L., 2007. Solid lipid nanoparticles: formulation factors affecting cell transfection capacity. Int. J. Pharm. 339, 261–268.

Doi, K., Hargitai, J., Kong, J., Tsang, S.H., Wheatley, M., Chang, S., Goff, S., Gouras, P., 2002. Lentiviral transduction of green fluorescent protein in retinal epithelium: evidence of rejection. Vis. Res. 42, 551–558.

Douglas, K.L., Piccirillo, C.A., Tabrizian, M., 2008. Cell line-dependent internalization pathways and intracellular trafficking determine transfection efficiency of nanoparticle vectors. Eur. J. Pharm. Biopharm. 68, 676–687.

Foerg, C., Ziegler, U., Fernandez-Carneado, J., Giralt, E., Rennert, R., Beck-Sickinger, A.G., Merkle, H.P., 2005. Decoding the entry of two novel cell-penetrating peptides in HeLa cells: lipid raft-mediated endocytosis and endosomal escape. Biochemistry 44, 72–81.

Freitas, C., Müller, R.H., 1999. Correlation between long-term stability of solid lipid nanoparticles (SLN™) and crystallinity of the lipid phase. Eur. J. Pharm. Biopharm. 47, 125–132.

Hoekstra, D., Rejman, J., Wasungu, L., Shi, F., Zuhorn, I., 2007. Gene delivery by cationic lipids: in and out of an endosome. Biochem. Soc. Trans. 35, 68–71.

Kanatani, I., Ikai, T., Okazaki, A., Jo, J., Yamamoto, M., Imamura, M., Kanematsu, A., Yamamoto, S., Ito, N., Ogawa, O., Tabata, Y., 2006. Efficient gene transfer by pullulan-spermine occurs through both clathrin- and raft/caveolae-dependent mechanisms. J. Control. Release 116, 75–82.

Karmali, P.P., Chaudhuri, A., 2007. Cationic Liposomes as non-viral carriers of gene medicines: resolved issues, open questions, and future promises. Med. Res. Rev. 27, 696–722.

Kim, T.W., Kim, Y.J., Chung, H., Kwon, I.C., Sung, H.C., Jeong, S.Y., 2002. The role of non-ionic surfactants on cationic lipid mediated gene transfer. J. Control. Release 82, 455–465.

Li, W.H., Ishida, T., Tachibana, R., Almofti, M.R., Wang, X.Y., Kiwada, H., 2004. Cell type-specific gene expression, mediated by TFL-3, a cationic liposomal vector, is controlled by a post-transcription process of delivered plasmid DNA. Int. J. Pharm. 276, 67–74.

Liu, F., Yang, J., Huang, L., Liu, D., 1996. New cationic lipid formulations for gene transfer. Pharm. Res. 13, 1856–1860.

Liu, X.Y., Brandt, C.R., Rasmussen, C.A., Kaufman, P.L., 2007. Ocular drug delivery: molecules, cells,and genes. Can. J. Ophthalmol. 42, 447–454.

Lombardi Borgia, S., Regehly, M., Sivaramakrishnan, R., Mehnert, W., Korting, H.C., Danker, K., Roder, B., Kramer, K.D., Schafer-Korting, M., 2005. Lipid nanoparticles for skin penetration enhancement-correlation to drug localization within the particle matrix as determined by fluorescence and parelectric spectroscopy. J. Control. Release 110, 151–163.

Mannisto, M., Ronkko, S., Matto, M., Honkakoski, P., Hyttinen, M., Pelkonen, J., Urtti, A., 2005. The role of cell cycle on polyplex-mediated gene transfer into a retinal pigment epithelial cell line. J. Gene Med. 7, 466–476.

Mehnert, W., Mader, K., 2001. Solid lipid nanoparticles—production, characterization and applications. Adv. Drug Deliv. Rev. 47, 165–196.

Min, S.H., Molday, L.L., Seeliger, M.W., Dinculescu, A., Timmers, A.M., Janssen, A., Tonagel, F., Tanimoto, N., Weber, B.H.F., Molday, R.S., Hauswirth, W.W., 2005. Prolonged recovery of retinal structure/function after gene therapy in an Rs1h-deficient mouse model of X-linked juvenile retinoschisis. Mol. Ther. 12, 644–651.

Mortimer, I., Tam, P., MacLachlan, I., Graham, R.W., Saravolac, E.G., Joshi, P.B., 1999. Cationic lipid-mediated transfection of cells in culture requires mitotic activity. Gene Ther. 6, 403–411.

Olbrich, C., Bakowsky, U., Lehr, C.M., Muller, R.H., Kneuer, C., 2001. Cationic solid-lipid nanoparticles can efficiently bind and transfect plasmid DNA. J. Control. Release 77, 345–355.

Pelkmans, L., Helenius, A., 2002. Endocytosis via caveolae. Traffic 3, 311–320.

Pitkanen, L., Pelkonen, J., Ruponen, M., Ronkko, S., Urtti, A., 2004. Neural retina limits the nonviral gene transfer to retinal pigment epithelium in an in vitro bovine eye model. AAPS J., 6.

Pujals, S., Fernandez-Carneado, J., Ludevid, D., Giralt, E., 2008. D-SAP: a new, non-cytotoxic and fully protease resistant cell-penetrating peptide. Chem. Med. Chem. 3, 296–301.

Rejman, J., Oberle, V., Zuhorn, I.S., Hoekstra, D., 2004. Size-dependent internalization of particles via the pathways of clathrin-and caveolae-mediated endocytosis. Biochem. J. 377, 159–169.

Rejman, J., Bragonzi, A., Conese, M., 2005. Role of clathrin- and caveolae-mediated endocytosis in gene transfer mediated by lipo- and polyplexes. Mol. Ther. 12, 468–474.

Rejman, J., Conese, M., Hoekstra, D., 2006. Gene transfer by means of lipo- and polyplexes: role of clathrin and caveolae-mediated endocytosis. J. Liposome Res. 16, 237–247.

Ruponen, M., Ronkko, S., Honkakoski, P., Pelkonen, J., Tammi, M., Urtti, A., 2001. Extracellular glycosaminoglycans modify cellular trafficking of lipoplexes and polyplexes. J. Biol. Chem. 276, 33875–33880.

Salvati, A., Ciani, L., Ristori, S., Martini, G., Masi, A., Arcangeli, A., 2006. Physico-chemical characterization and transfection efficacy of cationic liposomes containing the pEGFP plasmid. Biophys. Chem. 121, 21–29.

Subramanian, A., Ranganathan, P., Diamond, S.L., 1999. Nuclear targeting peptide scaffolds for lipofection of nondividing mammalian cells. Nat. Biotechnol. 17, 873–877.

Tabatt, K., Kneuer, C., Sameti, M., Olbrich, C., Muller, R.H., Lehr, C.M., Bakowsky, U., 2004. Transfection with different colloidal systems: comparison of solid lipid nanoparticles and liposomes. J. Control. Release 97, 321–332.

Thomas, P., Smart, T.G., 2005. HEK293 cell line: a vehicle for the expression of recombinant proteins. J. Pharmacol. Toxicol. Methods 51, 187–200.

Tseng, W.C., Haselton, F.R., Giorgio, T.D., 1999. Mitosis enhances transgene expression of plasmid delivered by cationic liposomes. Biochim. Biophys. Acta 1445, 53–64.

von Gersdorff, K., Sanders, N.N., Vandenbroucke, R., De Smedt, S.C., Wagner, E., Ogris, M., 2006. The internalization route resulting in successful gene expression depends on polyethylenimine both cell line and polyplex type. Mol. Ther. 14, 745–753.

Zabner, J., Fasbender, A.J., Moninger, T., Poellinger, K.A., Welsh, M.J., 1995. Cellular and molecular barriers to gene-transfer by a cationic lipid. J. Biol. Chem. 270, 18997–19007.

Zuhorn, I.S., Kalicharan, R., Hoekstra, D., 2002. Lipoplex-mediated transfection of mammalian cells occurs through the cholesterol-dependent clathrin-mediated pathway of endocytosis. J. Biol. Chem. 277, 18021–18028.